Aquat. Living Resour. 13 (2000) 275–281

S0990744000010809/FLA

Observation and explanation of systematic split-beam angle measurement errors

Robert Kieser[a]*, Timothy Mulligan[a], John Ehrenberg[b]

[a] *Pacific Biological Station, Department of Fisheries and Oceans, Hammond Bay Road 3190, Nanaimo, BC V9R 5K6, Canada*

[b] *Hydroacoustic Technology Inc., 755 NE Northlake Way, Seattle, WA 98112, USA*

Accepted 20 March 2000

Abstract – Experiments conducted at the Qualark Creek acoustic site on the Fraser River have shown unexpected systematic errors in the split-beam angle measurement. A tethered dead salmon with a target strength of approximately –30 dB was used as a target at 3.7 m range. A signal-to-noise ratio of ~12 dB was observed. This target strength and signal-to-noise ratio are typical in some rivers where migrating adult salmon are observed. The target's location was measured both from the frame used to position the target in the beam and from the acoustic data. Comparison of these two sets of measurements demonstrated a bias that increased with the target's distance off the beam axis. The acoustically measured target locations were closer to the beam axis than the actual locations. Each acoustic estimate represented the mean location obtained after 3 000 pings. Results from a simulation model that includes the effects of random noise on the split-beam angle measurement reproduce the systematic underestimate of these angles. This bias increases rapidly with increasing off-axis target location and decreasing signal-to-noise ratio. The bias has been observed for circular and elliptical beams and the model accurately predicts the magnitude and direction of the systematic part of the angle measurement error in both cases. Results for a circular transducer are used here to illustrate the situation. The presence of this bias can affect measurements of fish density and migration speed. At the low signal-to-noise ratios often obtained in riverine environments, those who use a split-beam system for observation or estimation of fish should be aware of this phenomenon.

hydroacoustic / split-beam / angle measurement bias / TS measurement

Résumé – Observation et explication des erreurs systématiques de mesure d'angle de sonar. Des expériences conduites sur le site de Qualark Creek sur le fleuve Fraser ont montré des erreurs systématiques imprévues dans la mesure d'angle du sonar. Un saumon mort dont l'indice de réflexion était d'environ –30 dB a été placé comme cible à 3,7 m. Le rapport signal/bruit observé était de 12 dB environ. Ces indices de réflexion et rapport signal/bruit sont typiques dans certains fleuves où sont observés des saumons adultes en migration. La position de la cible a été mesurée à la fois à partir du cadre utilisé pour positionner la cible dans le faisceau et à partir des données acoustiques. Des comparaisons de ces deux séries de mesures ont démontré un biais qui augmentait avec l'éloignement de l'axe du faisceau. La localisation des cibles mesurée acoustiquement est plus proche de l'axe du faisceau que la position réelle. Chaque estimation acoustique représente la localisation moyenne obtenue après 3 000 impulsions. Les résultats d'un modèle de simulation, qui inclut les effets du bruit de façon aléatoire sur les mesures d'angle du sondeur, reproduisent la sous-estimation systématique de ces angles. Ce biais augmente rapidement avec l'éloignement des cibles de l'axe et la diminution du rapport signal/bruit. Le biais a été observé avec des faisceaux circulaires et elliptiques, et le modèle prévoit de façon précise l'amplitude et la direction de la partie systématique des erreurs de mesure d'angle dans les deux cas. Les résultats obtenus avec un transducteur circulaire sont utilisés ici pour illustrer la situation. La présence de ce biais peut affecter les mesures de densité des poissons et de vitesse de migration. Lors d'un faible rapport signal/bruit, souvent obtenu en rivière, il est recommandé de prêter attention à ce phénomène.

hydroacoustique / double faisceau / biais de mesure angulaire / indice de réflexion

**Correspondence and reprints.*
E-mail address: kieserr@pac.dfo-mpo.gc.ca (R. Kieser).

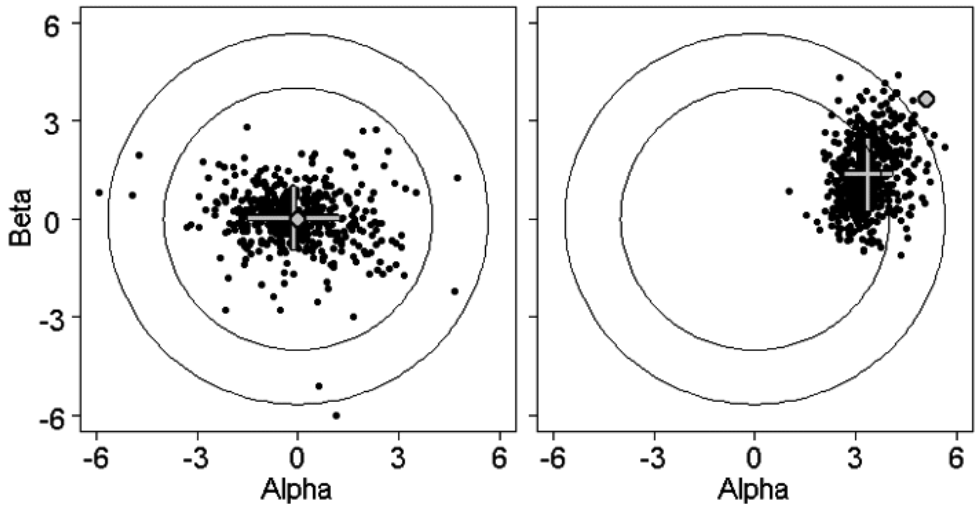

Figure 1. Actual and measured ping-by-ping target locations. The actual target locations are shown by a circle, split-beam positions are given by small dots and mean measured positions and standard deviations by a cross. Five hundred echoes from each target location are shown. The circles indicate the –3 and –6 dB one-way beam pattern factor for the 8° transducer.

1. INTRODUCTION

Split-beam echosounders have become a standard tool in fisheries and in underwater work where target location is important. Split-beam measurements provide the three-dimensional target location in the beam and hence allow target strength estimation (Traynor, 1986; Traynor and Ehrenberg, 1990) and tracking of individual fish in four dimensions (Brede et al. 1990).

Early measurements (Carlson and Jackson, 1980) were preceded by careful theoretical studies (Ehrenberg, 1979; Ehrenberg, 1981) that recommended a minimum signal-to-noise ratio of about 20 dB. The theoretical work and extensive laboratory measurements (Hood, 1987; Reynisson, 1987; Reynisson, 1990; Reynisson, 1998; Simmonds, 1990) have confirmed the accuracy of split-beam location and target strength measurements under high signal-to-noise conditions.

We have observed significant split-beam angle measurement biases under low signal-to-noise conditions in rivers. This paper compares the split-beam angle measurement bias with simulation results that provide a good explanation for the systematic part of the observed location errors.

2. METHODS

2.1. Target measurements

A target experiment was conducted at the Qualark Creek acoustic site, on the Fraser River, to compare known and measured target locations and other parameters. A frame was used to place a target at a known angular position in the acoustic beam. The acoustic system included a 200 kHz HTI 240 split-beam echosounder and an 8° transducer. Single-target echo information was recorded on a personal computer. Several target experiments were completed with a 10 cm diameter plastic sphere and a tethered dead salmon, both with a target strength of approximately –30 dB and at a range of 3.7 m. Based on this target strength and oscilloscope estimates of the mean noise power at the target range, the signal-to-noise was estimated as approximately 12 dB for on-axis targets. A similar signal-to-noise is typical for the adult salmon that generally are observed at slightly larger range. One of the tethered salmon experiments is used to illustrate the results.

Ping by ping split-beam angle measurements from two target locations are shown in *figure 1* and averaged measurements are in *figure 2*. Both figures show a systematic angle measurement bias. This bias will be unobserved if the true target locations are unknown. Experiments with different transducers, targets and echosounders were conducted at similarly low signal-to-noise ratios. All showed bias towards the beam axis in addition to the expected scatter of the measured target locations.

Following the elimination of procedural errors as a cause of this bias, we reviewed the classic conditions for accurate and interference-free sonar observations. These conditions include:

– homogeneous media,
– the target echo precedes any surface or bottom reverberation,
– target is located in the far field of the transducer,
– target is a 'point-source target',
– high signal-to-noise ratio.

The repeatability and symmetry of our observations guided us to examine the signal-to-noise ratio as a

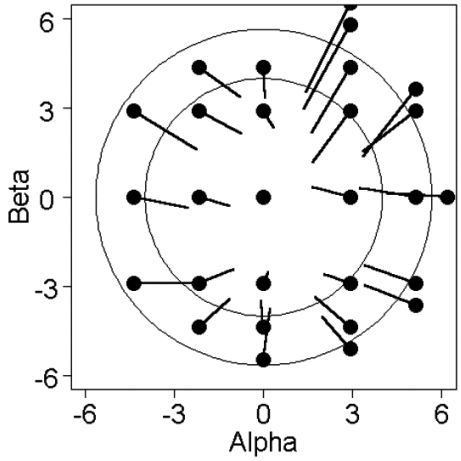

Figure 2. Actual and average measured target locations. Actual target locations are shown by a dot. Short lines connect the actual and observed locations. The circles indicate the –3 and –6 dB one-way beam pattern factor for the 8° transducer. Average measured locations are based on the echoes from 3 000 pings.

possible cause of the observed bias. Development of a mathematical model and simulation software followed. An outline of the simulation is presented below, details will be published at a later date.

2.2. Split-beam simulation

The simulation follows the split-beam measurement process and the signal processing that have been described by MacLennan and Simmonds (1991) and Ehrenberg (1981).

The split-beam angle measurement is based on the following geometric relation,

$$\sin(a_m) = \omega \cdot a_e / d \tag{1}$$

where a_m and a_e are the mechanical and electrical angle, respectively, ω is the angular frequency of the echo, and d gives the distance between the effective centres of the transducer halves. The electrical angle is given by the phase difference of the incoming wave between the effective centres of the transducer halves. The mechanical angle gives the direction to the target relative to the acoustic axis. Generally two angles (up/down and left/right) are measured.

Simulation of the electrical angle between transducer halves starts with generating the real and imaginary part of the (target) signal for each transducer quadrant,

$$a_{cqj} = A_j \cdot \cos(\phi_{qj}) \tag{2}$$

$$a_{sqj} = A_j \cdot \sin(\phi_{qj})$$

where a_{cqj} and a_{sqj} are the real and imaginary part from quadrant q and echo j, and the signal amplitude and phase are A_j and ϕ_{qj}. A single amplitude and phase are used to describe each echo, since we restrict our simulation to isolated targets and to narrow band echo-sounders (Haykin, 1994; Ziemer and Tranter, 1995). We use A_j rather than A_{qj} as the quadrants are of the same size and are essentially at the same range, when considering spreading and absorption.

The signal amplitudes A_j are obtained from,

$$A_j = 1/2 \cdot T_j \cdot Df_j \cdot Dq_j \tag{3}$$

where T_j are the Rayleigh distributed signal amplitudes and Df_j and Dq_j are the full and quadrant beam directivity functions (Clay and Medwin, 1977). The factor of 1/2 is used since each quadrant receives only 1/4 of the signal power. The signal phase ϕ_{qj} is given by the target location relative to the transducer beam axis and the appropriate quadrant centre.

Independent Rayleigh distributed noise amplitudes N_{qj} are generated for each quadrant. The noise power on the full beam is set to one and quadrant beam noise power to 1/4, which accounts for the incoherent addition of the noise from the quadrants. Independent, uniformly distributed noise phases φ_{qj} are generated for each quadrant. The summed signal and noise is obtained as follows:

$$a_{cqj} = A_j \cdot \cos(\phi_{qj}) + N_{qj} \cdot \cos(\varphi_{qj}) = A'_{qj} \cdot \cos(\phi'_{qj}) \tag{4}$$

$$a_{cqj} = A_j \cdot \sin(\phi_{qj}) + N_{qj} \cdot \sin(\varphi_{qj}) = A'_{qj} \cdot \sin(\phi'_{qj})$$

The last part of the relation indicates that the combined signal and noise can be expressed by a single amplitude A'_{qj} and phase ϕ'_{qj} for each quadrant.

The simulation then combines the quadrant signals to form the up/down and left/right half-beam and the sum-beam outputs. Only signals with a sum-beam amplitude that exceeds the sum-beam threshold are accepted. The accepted signals are used to estimate the angular location (equation 1), directivity and amplitude of the simulated echo from the target. A directivity (beam pattern) threshold now eliminates targets with small estimated directivity or equivalently targets with large estimated position angles. Finally, given a series of simulated echoes for a target at a fixed position, mean and standard deviation of the acoustically measured position, directivity, target size, etc. are calculated. The detection probability for the target is estimated by dividing the number of detected echoes by the number of generated (transmitted) pings.

2.3. Simulation parameters

The simulation uses the following major parameters:

– known target location measured in split-beam angles α and β,

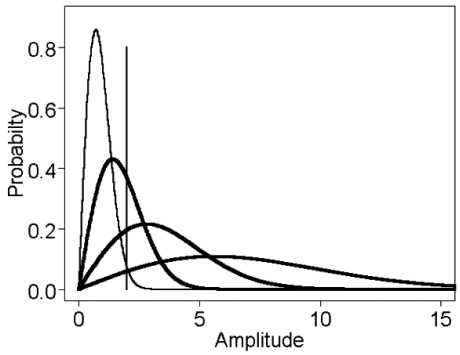

Figure 3. Rayleigh distributions for signal and noise. The light solid line gives the sum-beam noise amplitude distribution. The heavy lines give sum-beam signal amplitude distributions with 6, 12 and 18 dB signal-to-noise. The vertical line indicates a threshold-to-noise ratio of 6 dB or given a mean noise power one a sum-beam threshold of 2 V. An on-axis target with 18 dB signal to noise will yield 12 or 6 dB amplitude distributions when it is located in off-axis positions with –3 or –6 dB one-way beam pattern factor.

– frequency (Hz),
– sound speed in water ($m \cdot s^{-1)}$,
– full beamwidth X and Y (degrees),
– signal-to-noise ratio (dB),
– threshold-to-noise ratio (dB),
– beampattern threshold (dB).

The split-beam angles α and β, frequency, sound speed and beamwidth require little explanation. The signal-to-noise ratio (SNR) is defined as on-axis target sum-beam signal power over sum-beam noise power. The simulation always used a sum-beam noise power of one. The SNR thus defines the relative target size. Spreading, absorption and TVG are not required, because all signals are referred to the transducer face. The threshold-to-noise ratio (TNR) is defined as sum-beam threshold power level over noise power. It gives the sum-beam threshold that is used to eliminate small echoes, which are likely to be dominated by noise. Finally, the beam pattern threshold (BPT) is used to eliminate targets with large estimated off-axis locations that correspond to beam pattern factors below a specified value.

3. SIMULATION RESULTS

Figure 3 shows Rayleigh distributed noise and signal amplitude probability density functions in relation to a typical sum-beam threshold. Simulated sum-beam signal plus noise amplitude distributions for a signal-to-noise ration of 12 dB and target position of 0, 2 and 4° are shown in *figure 4*. At this signal-to-noise, a substantial portion of the low end of the distribution is removed by the sum beam threshold.

Figures 5 and *6* give the individual and average simulated target positions, respectively. The simulation parameters are given in *figure 5*. A systematic bias towards the beam axis is apparent. A summary of the split-beam angle measurement bias and standard deviation is given in *figure 7*. From top to bottom, the four lines correspond to 6, 12, 18 and 24 dB SNR. Both angle measurement bias and standard deviation increase with decreasing SNR and become significant at low SNR.

Figure 8 explains the primary reason for the split-beam angle measurement bias. The lower left and the upper panel shows histograms of the sum-beam noise amplitude and the phase difference between transducer halves, respectively. The plot of sum-beam noise amplitude versus phase difference between transducer halves shows that noise signals that exceed the sum-beam threshold have a tendency to be located near the beam axis. At low SNR, this tendency will be imposed on the estimated target location. The bias will increase with off-axis target location, since the effective SNR will be lower.

A secondary reason for the split-beam angle measurement bias is found in the beam pattern threshold that is used by typical split-beam systems and our simulation. Targets that exceed the sum-beam threshold will also have to exceed the beam pattern threshold before they are accepted. Typically, targets that appear

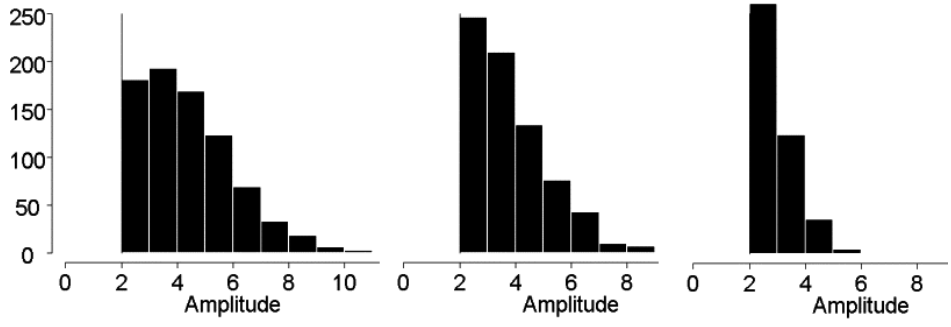

Figure 4. Simulated signal-plus-noise amplitude histograms for an 8° transducer and known off-axis target angles of 0, 2 and 4°. These angles correspond to beam pattern factors of 0, –0.75 and –3 dB. Data are from 1 000 simulated pings with mean noise power one, signal-to-noise ratio 12 dB, threshold to noise ratio 6 dB (vertical line) and beampattern threshold –10 dB.

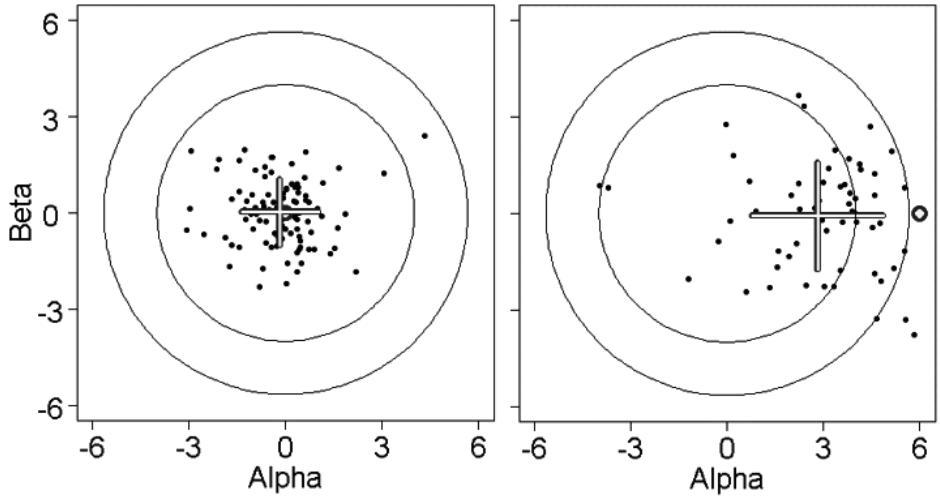

Figure 5. Simulated target positions for known off-axis target locations of 0 and 6° (large dot). Echoes are shown by a small dot and average measured locations and their standard deviations by a cross. This, and the following simulations are for an 8° transducer, mean noise power one, signal-to-noise ratio 12 dB, threshold to noise ratio of 6 dB, beampattern threshold –10 dB and 1 000 pings. The circles indicate the –3 and –6 dB one-way beam pattern factor.

at large off axis angles are removed, generating an additional bias towards the beam axis. However, it is important to note that these effects are negligible under reasonable signal-to-noise conditions and that an understanding of the measurement process will allow us to improve the results.

4. DISCUSSION

A split-beam angle measurement bias has been observed at low signal-to-noise ratios and a simulation model is described that explains the major experimental results. We find that the angle measurement bias increases as the target moves off-axis (decreasing beam pattern factor) and that the scatter in the measured positions is relatively independent of off-axis position. However, both increase with decreasing SNR (*figure 7*). The model also correctly predicts the observed detection probability.

Several experiments with a plastic sphere target and tethered salmon were completed. Both had the same

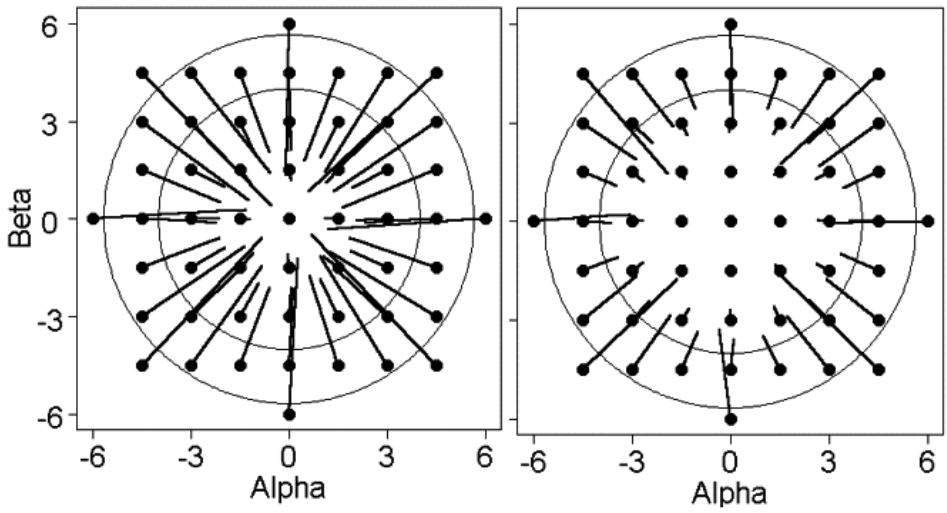

Figure 6. Simulated average target positions for 6 and 12 dB signal-to-noise ratio. Short lines connect the actual and simulated locations. The circles indicate the –3 and –6 dB one-way beam pattern factor. Simulation parameters are given in *figure 5*.

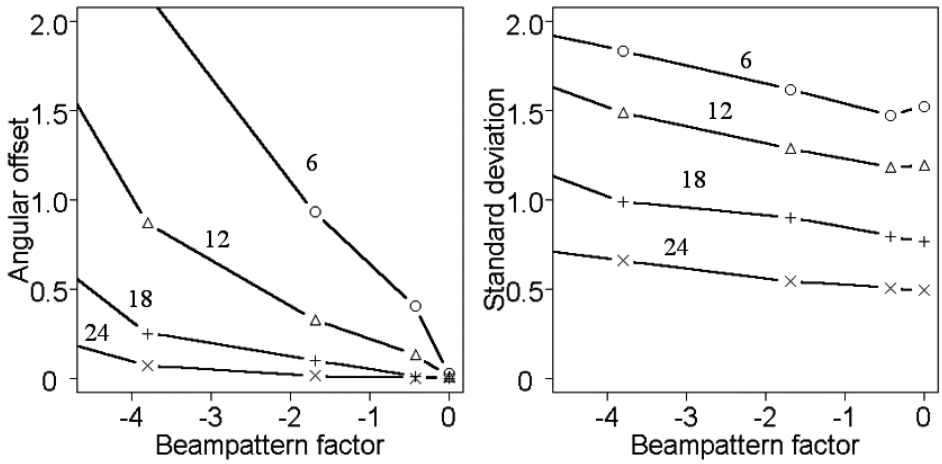

Figure 7. Simulated split-beam angle measurement bias (angular offset) and standard deviation for 6, 12, 18 and 24 dB signal-to-noise ratio as a function of target location (beampattern factor). Both bias and standard deviation increase as the target moves off axis (decreasing beam pattern factor). The scatter in the simulated positions is relatively independent of off-axis position. Simulation parameters are given in *figure 5*.

target strength and signal-to-noise and generated similar results. An example of the latter is reported here.

The simulation results shown here are for an 8° transducer, signal-to-noise ratio of 12 dB, threshold-to-noise ratio of 6 dB and beampattern threshold of –10 dB. These parameters have been chosen to approximate the conditions of experiments. A comparison of the measurements (*figures 1* and *2*) and the

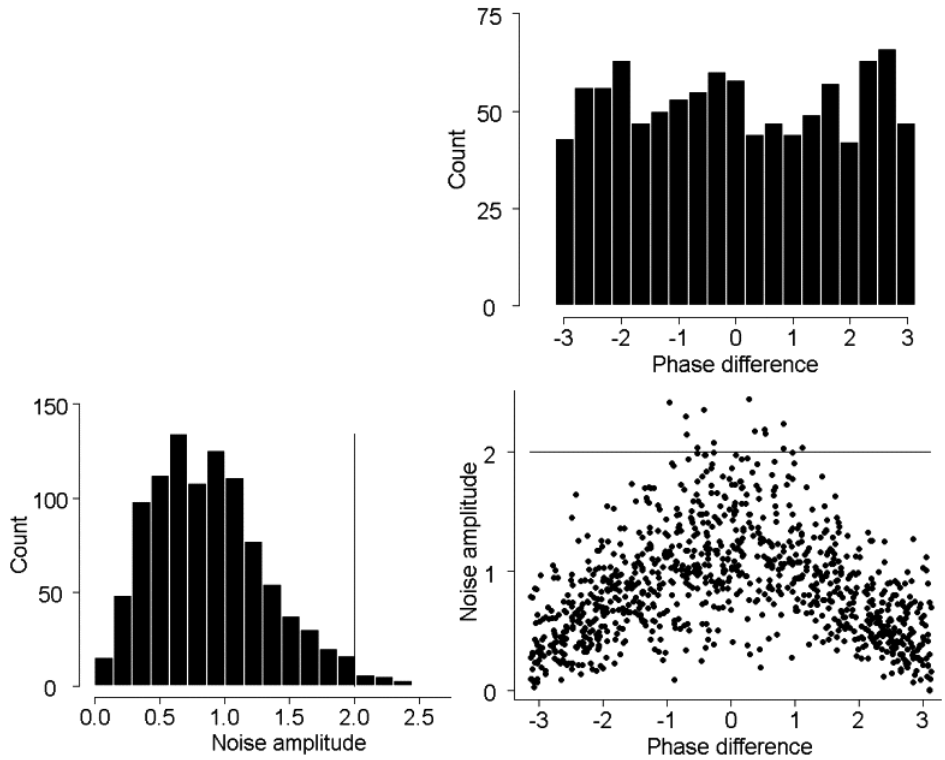

Figure 8. Explanation for split-beam angle measurement bias. Simulated sum-beam noise amplitude histogram with mean power one and histogram of phase difference between transducer halves. The horizontal line indicates a sum-beam threshold of 2 V. The plot of noise amplitude versus phase difference illustrates that the larger noise signals that are likely to exceed the sum-beam threshold are preferentially associated with small off-axis angles. This trend will be significant in estimating target location form signals that have a large noise component.

simulation results (*figures 5* and *6*) show that the simulation provides a good explanation for the observed split-beam angle measurement bias.

Given fixed targets and a reasonable number of simulated observations for each target (e.g. 1 000), the simulation will tend to generate a symmetric pattern for the target location bias (*figure 6*), we are therefore looking for an explanation for the asymmetry shown in the experiment (*figure 2*).

In practice, the split-beam angle measurement bias will translate to biased measurements of the angular position of fish targets. For fixed-position observations, this will lead to an underestimation of fish swimming speed and an overestimation of fish density. Work is in progress to investigate the effect of this bias on detection probability, target strength and other split-beam measurements. We feel that the model presented here increases our understanding of the split-beam measurement process and will stimulate the development of improved ways of dealing with the data to produce even better results especially under difficult conditions.

References

Brede, R., Kristensen, F.H., Solli, H., Ona, E., 1990. Target tracking with a split beam echo sounder. Int. Symp. on Fish. Acoustic, June 22–26, Seattle, WA, USA. Rapp. P.-v. Réun. Cons. Int. Explor. Mer 189, 254–263.

Carlson, T.J., Jackson, D.R., 1980. Empirical evaluation of the feasibility of split-beam methods for direct in situ target strength measurement of single fish. Rep. Appl. Phys. Lab. Univ. Wash. APL-UW 8006.

Clay, C.S., Medwin, H., 1977. Acoustical oceanography: principles and applications. John Wiley & Sons, New York.

Ehrenberg, J.E., 1979. A comparative analysis of in situ methods for directly measuring the acoustic target strength of individual fish. IEEE J. Ocean Engin. 4, 141–152.

Ehrenberg, J.E., 1981. Analysis of split-beam backscattering cross section estimation and single echo isolation. Rep. Appl. Phys. Lab. Univ. Wash., APL-UW 8108.

Haykin, S., 1994. Communication Systems. John Wiley & Sons, New York.

Hood, C.R., 1987. Measurements of a split-beam transducer. Int. Symp. Fish. Acoustic, June 22–26, 1986 Seattle, WA, USA, Mimeo.

MacLennan, D.N., Simmonds, E.J., 1991. Fisheries Acoustics. Fish and Fisheries Series. Chapman & Hall, London.

Reynisson, P., 1987. Measurements of the Beam Pattern and Compensation Errors of Split-Beam Echo Sounders. Int. Symp. on Fish. Acoustic, June 22–26 Seattle, WA, USA, Mimeo.

Reynisson, P., 1990. A geometric method for measuring the equivalent beam angles of hull mounted transducers. Int. Symp. on Fish. Acoustic, June 22–26, Seattle, WA, USA. Rapp. P.-v. Réun. Cons. Int. Explor. Mer. 189, 176–182.

Reynisson, P., 1998. Monitoring of equivalent beam angles of hull-mounted acoustic survey transducers in the period 1983–1995. ICES J. Mar. Sci. 55, 1125–1132.

Simmonds, E.J., 1990. Very accurate calibration of a vertical echosounder: A five year assessment of performance and accuracy. Int. Symp. on Fish. Acoustic, June 22–26, Seattle, WA, USA. Rapp. P.-v. Réun. Cons. Int. Explor. Mer. 189, 183–191.

Traynor, J.J., 1986. Some preliminary results using a new split-beam/dual-beam target strength measurement system. ICES, C.M. 1986/B: Fish capture committee.

Traynor, J.J., Ehrenberg, J.E., 1990. Fish and standard sphere target strength measurements obtained with a split-beam/dual-beam system. Int. Symp. Fish. Acoustic, June 22–26 1990 Seattle, WA, USA. Rapp. P.-v. Réun. Cons. Int. Explor. Mer. 189, 325–335.

Ziemer, R.E., Tranter, W.H., 1995. Principles of communication systems, modulation and noise. John Wiley & Sons, New York.